Thin Solid Films 330 (1998) 14–20

Structure and solvation forces in confined films of alkanes

Marjolein Dijkstra[1]

CECAM, Ecole Normale Supérieure de Lyon, 46, Allée d'Italie, 69364 Lyon Cedex 07, France

Abstract

We compute by computer simulations the solvation force of a system of linear and branched alkanes confined in a slab geometry. The solvation force for linear decane oscillates with distance with a periodicity close to the width of the molecules. The branched alkanes, 2-methylundecane and 2-methylheptane, show a similar oscillatory behaviour, however the oscillations are decreased with a factor of about three and show a long-range attractive force. In addition, we show that the critical temperature of the liquid-vapour coexistence of n-pentane shifts to lower temperatures upon confining. © 1998 Elsevier Science S.A. All rights reserved

Keywords: Thin fluid films; Alkanes; Computer simulations; Solvation forces

1. Introduction

The stability of colloidal suspensions are well-described by mean-field theories like the Van der Waals theory or the Derjaguin Landau Verweij Overbeek theory in the case of charged-stabilised colloids [1,2]. However, when two big colloidal particles or surfaces approach each other closer than a few nanometers, these theories have been found to be inadequate to predict the interactions between the surfaces, as other forces will play a role [3]. These short-range forces are the solvation forces or hydration forces in the case of water and they can be measured experimentally by the surface force apparatus [3,4]. These short-range solvation forces are monotonically repulsive, monotonically attractive or oscillatory with distance. At high liquid densities these solvation forces show an oscillatory behaviour, while at low liquid densities a purely exponential decay is found, provided the liquid is sufficiently far from the critical point and no phase transition occurs.

The oscillatory behaviour of the solvation force is now well-understood for simple spherical molecules. Theoretical work and computer simulations of Lennard–Jones fluids and hard spheres show that the oscillatory solvation force originates from the stratification or ordering of the molecules in layers when the fluid is confined by the surfaces [5–18].

Whether the structure of the solvation force is oscillatory or monotonically decaying, depends also strongly on the chemical and physical nature of the surfaces, for example, whether they are hydrophilic, hydrophobic, smooth, corrugated, etc. On the other hand, the oscillatory behaviour is very sensitive for the detailed chemical structure of the molecules and the ability of the molecules to order. One of the most striking examples of this sensitivity is the difference between the solvation force of linear and branched alkanes. For example, experiments showed that a single methyl side group on a linear octadecane chain can completely eliminate the oscillations in the solvation force [19,20]. This phenomenon may be the reason why branched alkanes are better lubricants than linear ones. A similar difference was observed in force measurements of low molecular weight polymer melts. Unbranched polydimethylsiloxane (PDMS) exhibits a short-range oscillatory solvation force profile, while branched polybutadiene (PB) shows only a monotonically decaying solvation force which is long-ranged attractive [21,22]. However, recent computer simulations of octane and isooctane did not reveal this unexpected difference in the solvation force profiles [23]. Also recent experiments of 3-methylundecane show that the solvation force show still an oscillatory behaviour, however the amplitudes of the oscillations are smaller than for linear undecane [24]. A similar decrease in the amplitudes of the

[1] Present address: H.H. Wills Physics Laboratory, Royal Fort, Tyndall avenue, Bristol BS8 1TL, UK.

0040-6090/98/$ - see front matter
PII S0040-6090(98)00795-0

oscillations has been found in recent computer simulations of n-hexadecane and squalane [25].

In this article, we show by computer simulations that there is indeed a difference in the solvation force and structure for confined films of branched and unbranched alkanes. In Section 2, we explain our simulation method. In particularly, we explain our choice of ensemble and we derive an expression for the solvation force. In Section 3, we show the results of the simulations. Our results show an oscillatory behaviour for the solvation force of linear decane with a periodicity close to the width of the alkanes. For 2-methylundecane and 2-methylheptane, we still found oscillations in the solvation force, but the amplitudes of the oscillations are decreased with respect to n-decane. The solvation force, however, is shifted to the attractive region. In order to investigate whether our measurements were sufficiently far from the critical point, we located the liquid-vapour transition for the confined fluid. In Section 4, we show that the critical temperature of the liquid-vapour coexistence shifts to lower temperatures upon confining and that the density of the liquid in the simulations for the solvation force were sufficiently far from the critical point.

2. Simulations

The surface force apparatus measures the force between two molecularly smooth mica surfaces immersed in a fluid as a function of the distance. In the experiments, the solvation force is measured when a droplet is inserted between the plates. The droplet is macroscopically large and serves as a reservoir for the fluid between the plates, i.e. molecules can flow in and out the slit under a fixed chemical potential of the reservoir. In order to compute the solvation force in a simulation, we compute the force exerted on the plates by the fluid between the plates, while we keep the chemical potential fixed, i.e. we did simulations in the Grand canonical ensemble.

Below, we will describe the thermodynamics of this system in order to derive an expression of the solvation force (see [26] for more details). When we describe the thermodynamics of such an open system, we should consider the grand potential $\Omega = U - TS - \mu N$, where U is the internal energy, S the entropy, T the temperature, and N the number of particles. The change in the grand potential of this system is [26]:

$$d\Omega = -p^{\mathrm{b}} dV^{\mathrm{res}} - SdT - Nd\mu + 2\gamma dA - AfdH \tag{1}$$

where p^{b} is the bulk pressure, V^{res} is the volume of the whole reservoir, A the area of the plates, H the distance between the plates and f the solvation force. The plate-fluid interfacial tension γ is given by:

$$\gamma = \frac{1}{2}\left(\frac{\partial \Omega}{\partial A}\right)_{V,T,\mu,H} \tag{2}$$

The last two contributions are due to the confinement and depend on the area and the distance between the plates. We now consider the same reservoir with the same volume and chemical potential but without the plates:

$$d\Omega = -p^{\mathrm{b}} dV^{\mathrm{res}} - S^{\mathrm{b}} dT - N^{\mathrm{b}} d\mu \tag{3}$$

If we now define the surface excess functions

$$\Omega^{\mathrm{ex}} = \Omega - \Omega^{\mathrm{b}}$$

$$S^{\mathrm{ex}} = S - S^{\mathrm{b}} = 2As$$

$$N^{\mathrm{ex}} = N - N^{\mathrm{b}} = A\Gamma$$

we obtain

$$d\Omega^{\mathrm{ex}} = -2AsdT - A\Gamma d\mu + 2\gamma dA - AfdH \tag{4}$$

which is a function of the temperature, chemical potential, area and plate separation. The surface excess functions separate the surface terms from the bulk terms. For a bulk system, the grand potential $\Omega^{\mathrm{b}}(\mu, V, T)$ is equal to:

$$\Omega^{\mathrm{b}}(\mu, V, T) = -p^{\mathrm{b}}(\mu, T)V \tag{5}$$

as volume of the system is an extensive quantity. For a confined system, there is an additional contribution to the grand potential due to the surfaces, as the area of a single wall A is an additional extensive quantity.

$$\Omega(\mu, V, A, H, T) = -p^{b}(\mu, T)V + 2\gamma(\mu, H, T)A \tag{6}$$

If we now consider a confined volume $V = AH$, the grand potential of the whole system can be written as:

$$\Omega(\mu, A, H, T) = A(-p^{\mathrm{b}}(\mu, T)H + 2\gamma(\mu, H, T)) \tag{7}$$

such that in the limit $H \to \infty$, the grand potential contains only a bulk contribution, i.e.

$$\lim_{H\to\infty} \Omega = -p^{\mathrm{b}}AH \tag{8}$$

leading to the condition:

$$\lim_{H\to\infty} 2\gamma/H = 0 \tag{9}$$

This condition is satisfied as in the limit $H \to \infty$, $2\gamma \to \gamma_1 + \gamma_2$ is constant, where γ_1 and γ_2 are the interfacial tensions for the fluid with plate 1 and 2, respectively. If we now consider the surface excess functions $\Omega^{\mathrm{ex}} = 2\gamma A$, the differential of Ω^{ex} is:

$$d\Omega^{\mathrm{ex}} = 2\gamma dA + 2Ad\gamma \tag{10}$$

$$= 2\gamma dA + 2A\left[\left(\frac{\partial \gamma}{\partial \mu}\right)_{\mathrm{T,H}} d\mu + \left(\frac{\partial \gamma}{\partial T}\right)_{\mu,\mathrm{H}} dT + \left(\frac{\partial \gamma}{\partial H}\right)_{\mu,\mathrm{T}} dH\right] \tag{11}$$

This expression should be equal to Eq. (4), which leads to the following relations:

$$\Gamma = -2\left(\frac{\partial \gamma}{\partial \mu}\right)_{\mathrm{T,H}} \tag{12}$$

$$s = -\left(\frac{\partial \gamma}{\partial T}\right)_{\mu, \mathrm{H}} \tag{13}$$

$$f = -2\left(\frac{\partial \gamma}{\partial H}\right)_{\mu, \mathrm{T}} \tag{14}$$

In the limit $H \to \infty$, the interfacial tension $2\gamma \to$ constant, and hence, we find that $f \to 0$ for a semi-infinite system.

Using that $\Omega^{\mathrm{ex}} = 2\gamma \mathrm{A}$ and $\Omega^{\mathrm{b}} = -\mathrm{p}^{\mathrm{b}}V = -\mathrm{p}^{\mathrm{b}}AH$, we obtain

$$\gamma = \frac{1}{2A}[\Omega + p^{\mathrm{b}}AH] \tag{15}$$

and the solvation force reads

$$f = -\frac{1}{A}\left(\frac{\partial \Omega}{\partial H}\right)_{\mu, \mathrm{T}, \mathrm{A}} - p^{\mathrm{b}} = p^{*} - p^{\mathrm{b}} \tag{16}$$

For a system with a plate at $z = 0$ and $z = H$, the fluid-wall potential can be written as $V_{\mathrm{ext}}(z) = V_{\mathrm{s}}(z) + V_{\mathrm{s}}(H\text{-}z)$. The pressure p^* can now be computed as follows [27]:

$$p^{*} = \frac{1}{A}\left(\frac{\partial \Omega}{\partial H}\right)_{\mu, \mathrm{T}, \mathrm{A}} \tag{17}$$

$$= -\int_0^H dz \rho(z) \frac{\partial V_{\mathrm{ext}}(z)}{\partial H}$$

By symmetry, we find that the force on the upper surface is equal to the force on the lower surface:

$$p* = \int_0^H dz \rho(z) \frac{\partial V_{\mathrm{s}}(H-z)}{\partial z} = -\int_0^H dz \rho(z) \frac{\partial V_{\mathrm{s}}(z)}{\partial z} \tag{18}$$

From Eq. (16), we find that the solvation force can be computed by performing simulations for different plate separations at a fixed chemical potential, temperature and plate area. We therefore performed Grand canonical Monte Carlo (GCMC) simulations of alkanes between two plates, where the independent variables are the chemical potential, μ, the volume $V = AH$ and the temperature T. In order to obtain a fixed chemical potential, particles are exchanged with a fictitious infinitely large reservoir which contains an ideal gas of the same particles, i.e. the ideal alkane chains have internal energies [28].

The alkanes are modeled by the united atom approximation, where every CH_3 or CH_2 group is described as a single interaction site. The non-bonded dispersive interactions between these 'united atoms' of different molecules or within a molecule (when two atoms are more than four atoms apart) are described with a Lennard–Jones potential. The potential parameters of unlike bead interactions are calculated using the Lorentz–Berthelot rules $\epsilon_{\mathrm{ij}} = \sqrt{\epsilon_{\mathrm{i}}\epsilon_{\mathrm{j}}}$ and $\sigma_{\mathrm{ij}} = \sqrt{\sigma_{\mathrm{i}}\sigma_{\mathrm{j}}}$. In addition, we used fixed bond lengths, a harmonic bond angle bending and a torsion potential. The Lennard–Jones interactions are shifted and truncated at 13.8 Å [29].

The parameters for the potentials of the linear alkanes were derived from calculations of the vapour-liquid phase equilibria of n-alkanes by Smit et al. [30]. For the branched alkanes, we used the model of Wang et al. [23], which is based on Jorgensen's optimized potentials for liquid simulations (OPLS).

In our model, we confine the alkane fluid in the z-direction by two flat surfaces. In the vicinity of the surfaces, the alkanes experience a potential field due to the solid surfaces. In our simulations, we used a 9–3 wall-potential, which corresponds to the summation of the mean field atom-solid 10–4 potentials from different lattice planes of a solid consisting of Lennard–Jones particles [31]. The values of the parameters are taken from [32], where a simple 9–3 site-wall potential is introduced for a surface with some texture. However, in our calculations we ignore the corrugation of the surfaces and we used the smooth potential. For more detail on the precise values of the potential parameters, we refer the reader to [33].

Conventional Monte Carlo schemes are not sufficiently efficient to ensure rapid equilibration, as direct insertion of a flexible particle in a dense fluid almost always results in an overlap with one of the other chains in the fluid. For a faster equilibration of the alkanes, it is essential to use the configurational bias Monte-Carlo (CBMC) method [34]. In this method, we grow the alkane chains segment by segment in such a way that configurations with favorable energies are found. For more technical details on the implementation of the CBMC-method see [34,30].

Most runs consist of at least 10^8 cycles. In each cycle, an attempt is made to regrow a part of the polymer using the CBMC-method and a removal or insertion of a particle in the box is attempted. On average, once every two cycles, a random displacement and random rotation of a particle in the box is attempted and once every five cycles, a whole polymer is regrown at a random place in the box using the CBMC-method.

3. Results and discussion

We perform computer simulations in the Grand-Canonical ensemble of a system of decane, 2-methylheptane and 2-methylundecane. The fluid is confined by solid surfaces of 34×34 Å. The plate separations vary from 5 to 50 Å. In the x- and y-direction, we use periodic boundary conditions, such that an infinite, periodic system is simulated. In all the simulations the temperature T is fixed at a value of 298 K and the chemical potential is such that the density of the reservoir corresponds to a liquid phase of 0.717 ± 0.008 g/cm^3.

In Fig. 1, we plot the solvation force versus the distance H between the plates for n-decane 2-methylheptane and 2-methylundecane. For n-decane, we observe strong oscillations with a periodicity of 4–4.5 Å, which is close to the width of the alkane molecules.

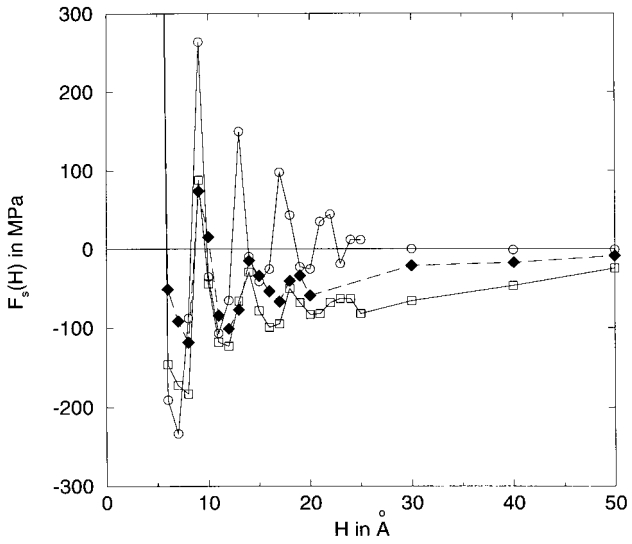

Fig. 1. The solvation force in MPa versus the distance H of the plates in Å for n-decane (open circles), 2-methylheptane (filled diamonds), and 2-methylundecane (open squares).

However, in the case of 2-methylheptane and 2-methylundecane, the oscillations are less pronounced and are shifted to the attractive region. At large plate separations, the solvation force for the branched alkanes goes to zero. At large plate distances the pressure exerted as the fluid between the plates is equal to the pressure exerted by the fluid outside the plates.

For 2-methylheptane the solvation force becomes zero at plate separations larger than 30 Å. For 2-methylundecane, we find that the solvation force approaches zero very slowly with increasing plate separation.

We also compute the density distribution $\rho(z)$ of n-decane at different values for the plate separation. No adsorption of alkanes are found for distances smaller than 5 Å. In Fig. 2a, we observe one fluid layer for a plate distance of 5–8 Å. For a separation of 9–12 Å (Fig. 2b), two layers are formed. Three layers are observed for a separation of 13–16 Å (Fig. 2c), four layers for distances of 17–21 Å (Fig. 2d), and five layers for distances of 22 Å (Fig. 2e). If we compare these density distributions with the solvation force, we observe clearly that one sharp peak at a distance of 5 Å corresponds with a high value for the solvation force. When we increase the distance we find that the density profile becomes broader: the solvation force drops, i.e. the fluid can be squeezed out easily. At a distance of 9 Å, we observe two sharp peaks corresponding with a high solvation force. By increasing the distance further the peaks become broader and the solvation force drops. At a distance of 13 Å, three well defined layers are formed: the solvation force is high. The solvation force decreases with increasing distance till at a distance of 17 Å a fourth layer appears. Again the two layers in the middle do not fit well and the solvation force increases when we increase the distance. At a distance of 18 Å, four sharp peaks are observed, etc. We can conclude that the origin of the oscillations in the solvation force lies in the stratification or ordering of the chains in layers. When the density distributions show sharp peaks, i.e. when the fluid orders in well-defined layers, the solvation force is high, i.e. it is difficult to squeeze out the fluid between the plates. The solvation force drops when the density distributions are broader, i.e. when it is difficult for the molecules to form well-defined layers. A similar behaviour it formed in the density profiles of 2-methylundecane. We plot for comparison the density profiles of n-decane and 2-methylundecane in Fig. 3, when one, two three and four well defined layers are formed between the plates. We took the density profiles at the maxima of the oscillations. We observe that the profiles of decane are more strongly peaked than those of 2-methylundecane. We also plot the density profiles for the end methyl groups of 2-methylundecane. We observe from these density profiles that one branched methylgroup is in the fluid layer, while the other lies between the fluid layers.

In Fig. 4, we show a typical configuration of a layer of n-decane at $H = 5$ Å. The density of this film is close to the bulk liquid density of n-decane and the alkanes are disordered in position and orientation. We therefore conclude that the configuration is fluid-like. In Figs. 5 and 6 typical snapshots are shown of n-decanes and 2-methylundecanes adsorbed in a slit with a slitwidth of 9 Å, and 13Å (n-decane) and 14 Å (2-methylundecane), respectively. We clearly see that discrete fluid layers are formed in the case of n-decanes, while the fluid is more homogeneous in the case of 2-methylundecane.

If we compare our results with the experimental data of

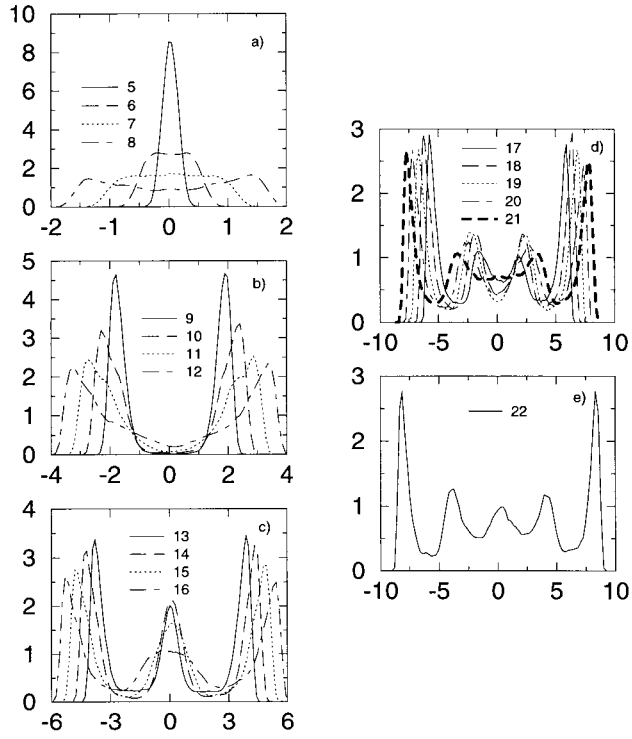

Fig. 2. Density distribution $\rho(z)$ in g/cm^3 of n-decane at different values for the plate separation (a) 5–8 Å, (b) 9–12 Å, (c) 13–16 Å, (d) 17–21 Å and (e) 22 Å. The plate separation in Å is written in the figures.

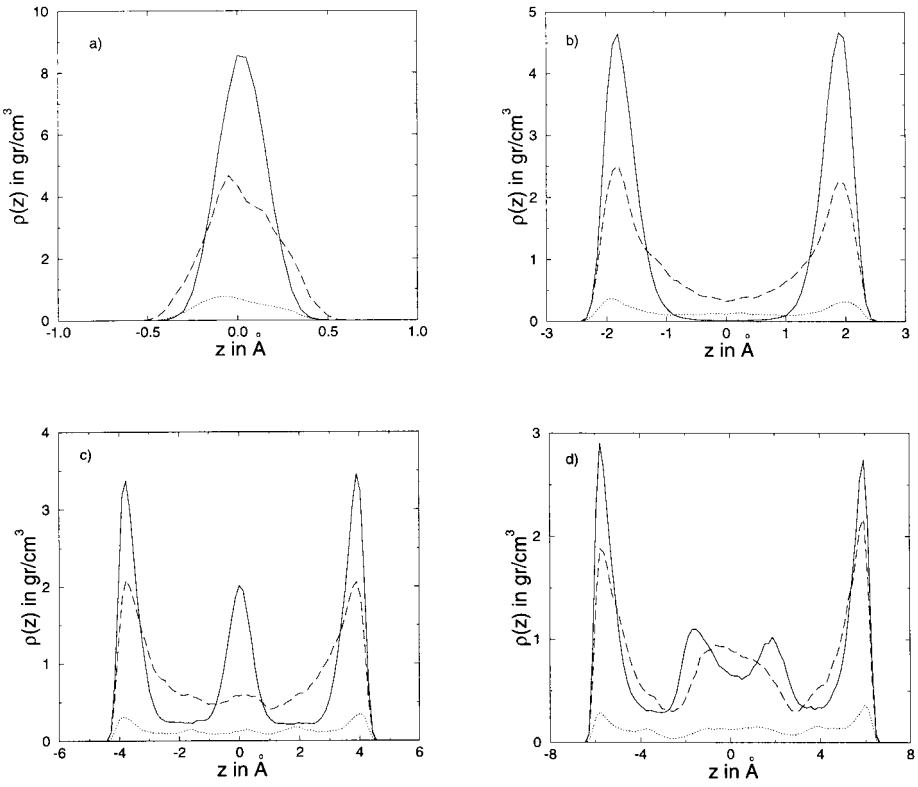

Fig. 3. Density distribution $\rho(z)$ in g/cm^3 of n-decane (solid line) and 2-methylundecane (dashed line) and that of the end methyl groups of 2-methylundecane (dotted line) versus z in Å for a plate separation of (a) 5 Å, (b) 9 Å, (c) 13 Å for n-decane and 14 Å for 2-methylundecane, and (d) 17 Å for n-decane and 18 Å for 2-methylundecane.

[19,24], we observe two remarkable features. Firstly, we still find oscillations in the solvation force of branched alkanes. We already mentioned that the origin of oscillations in the solvation force lies in the ordering of the molecules in fluid layers. In the case of n-decane, well-defined fluid layers are formed. However, the ability of branched alkanes to form discrete layers is reduced due to simple packing arguments, but is not completely eliminated, as can be seen in Figs 3, 5 and 6. This explains the two or three times weaker oscillations in our results in the case of branched alkanes, which agrees well with Granick's experiments of 3-methylundecane and linear undecane and with the simulation results of Gao [25].

The other surprising feature in our results is that the solvation force of branched alkanes is shifted to the attractive region. In Fig. 1, we see clearly that this shift in the solvation force for 2-methylheptane is still present for plate separations larger than 30 Å. This shift is even more pronounced for 2-methylundecane, while for linear decane the solvation force is already zero. From the density profiles of Fig. 3, we can understand why the branched alkanes exhibit a predominantly attractive force between the plates. The reason is that repulsive contributions to the solvation force stem only from particles close to the wall, i.e. $-\partial V_s(z)/\partial z > 0$ when $z < 2.6395$ Å. Thus, a repulsive solvation force can only be obtained when there is a strong ordering of molecules close to the wall. In Fig. 3, we find that in the case of branched alkanes, the ordering of the molecules close to the wall is smaller in comparison with n-decanes. The branched methyl groups frustrate the packing of the molecules in the layer close to the wall and the molecules will have a tendency to leave this layer. The amount of

Fig. 4. Typical snapshot of n-decane (xy-plane) at a plate separation of 5 Å (top view).

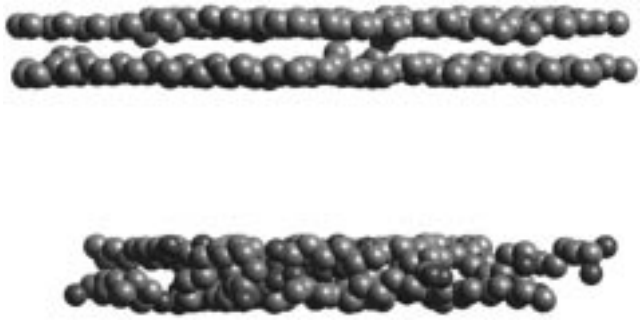

Fig. 5. Typical snapshots of n-decane (top) and 2-methylundecane (bottom) at a plate separation of 9 Å (side view).

interdigitation, i.e. in what extent individual molecules go from one layer to another, increases in the case of branched alkanes. This effect is already shown in [35], where molecules with many side branches (like squalane) reveal a large amount of interdigitation near a single wall. These bridges between the individual layers may be a reason for this long-range attractive force. This attractive solvation force agrees well with the experiments of Israelachvili et al. [3,4,19]. They observe a long-range attractive force up to a plate separation of 40 Å. As the amount of interdigitation varies for different branched alkanes, the resulting shift of the solvation force varies as well. This explains why we find a different shift for the solvation force for 2-methylheptane and 2-methylundecane for plate separations up to 50 Å.

In the simulations of Wang et al. [23] no remarkable difference is found in the solvation force between linear octane and branched iso-octane. However, in the simulations of Wang et al. [23] the molecules could flow in and out the slab and could evaporate and condensate in order to mimic a liquid droplet in a slit that is in equilibrium with its vapour. The resulting alkane density is hence 0.55–0.60 g/cm^3 in the slit, which is in the metastable region of the liquid-vapour coexistence. They also found a large tendency of the molecules to leave the slit. In order to overcome this problem, they used a penalty function, such that a part of the fluid remains in the pore.

4. Pore condensation

In order to investigate if the state points for measuring the solvation force were sufficiently far from the critical point, we located the liquid-vapour coexistence region for the confined fluid. In order to characterise possible phase equilibria in confined systems, we should ensure that the grand potential Ω_α^{ex} for phase α is equal to Ω_β^{ex} for phase β. As $\Omega^{ex} = \gamma A$, this condition can be rephrased as $\gamma_\alpha = \gamma_\beta$ when the area of the plates is kept constant. From Eq. (4), we observe that Ω^{ex} is a function of μ, T, A and L. One possible scenario for investigating phase transitions in a pore is to increase the chemical potential at fixed wall area, temperature, and plate separation. By measuring the adsorption isotherm, i.e. the density in the pore as a function of the chemical potential, one should be able to locate the phase transition. However, due to hysteresis, this procedure is very inaccurate in the determination of the phase coexistence points. A better route to locate phase coexistence is to perform Gibbs ensemble simulations. An extensive derivation of the Gibbs ensemble simulation technique applied for confined systems is given by Panagiotopoulos [12]. However, intuitively, one can understand this as follows. In an ordinary Gibbs ensemble simulation, volume and particles are exchanged between two systems until the volumes and numbers of particles of the separate systems reach stationary values within fluctuations. The resulting systems are those of two coexisting phases at the same pressure due to volume exchange and chemical potential due to particle exchange. In a Gibbs ensemble simulation for confined systems, area and particles are exchanged between the two systems, while the plate separation is kept constant. The exchange of particles ensures equal chemical potential for both phases, while the exchange of area ensures equal fluid-surface interfacial tension in the same spirit as the exchange of volume serves for equal pressure in bulk systems.

We performed Gibbs ensemble simulations for linear pentane for a plate separation of 9, 13, and 17 Å in order to locate the vapour-liquid coexistence region. The results are shown in Fig. 7. The results for the bulk are taken from [30]. We observe that the critical temperature shifts to lower temperatures with decreasing plate separation. This shift of the critical temperature of the liquid-vapour coexistence to lower temperatures upon confining is generic and is explained in [36]. The variable $1/H$ plays a similar role as the temperature. Since Van der Waals, it is known that attraction *between* the molecules is responsible for the liquid-vapour transition. When the temperature rises the attraction between the molecules decreases and above a certain temperature (the critical temperature) the liquid-vapour coexistence disappears, as the attraction is not sufficient enough anymore to cause phase separation. When a fluid is confined between two plates, the attraction between the molecules is diminished as the number of neighbours decreases. Already at lower temperatures the liquid-vapour

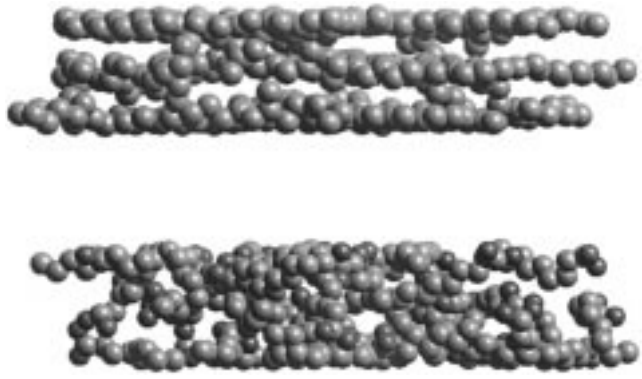

Fig. 6. Typical snapshots of n-decane (top) and 2-methylundecane (bottom) at a plate separation of 13 Å for n-decane and 14 Å for 2-methylundecane.

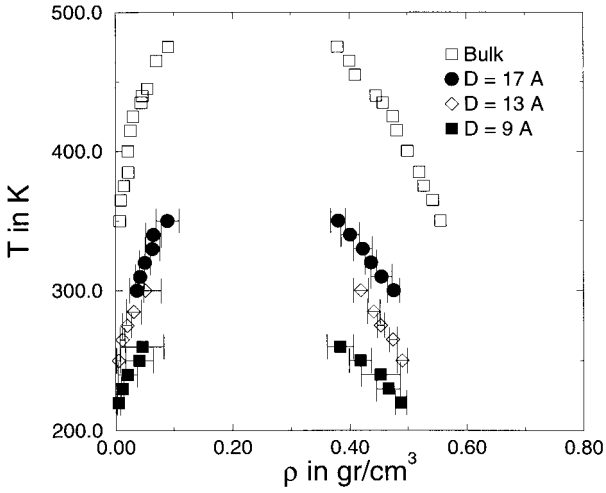

Fig. 7. Liquid-vapour coexistence points obtained from Gibbs ensemble Monte-Carlo simulations for n-pentane at a plate separation of 9, 13, and 17 Å. The results for the bulk are taken from [30].

region disappears, which results in a lower critical temperature. Note that we can neglect here at a first approximation the influence of the attractive walls as the walls are the same for the liquid and vapour phase.

For longer alkanes the critical temperature will also shift to lower temperatures upon confining, as this phenomena is generic. We therefore can conclude that our simulations for measuring the solvation force were sufficiently far from the critical point and the occurrence of any phase transition.

5. Conclusions

We performed Monte-Carlo simulations in the Grand canonical ensemble of a confined system of n-decane, 2-methylheptane and 2-methylundecane. We computed the solvation force exerted by the fluid on the plates. We found a large difference in the solvation force for linear and branched alkanes. For n-decane, we found an oscillatory behaviour in the solvation force with periodicity close to the width of the molecule. For the branched molecules, we found that the oscillations are decreased and are shifted to the attractive region, which might be the result of interdigitation that bridges the molecular layers formed in the fluid.

In addition, we computed the liquid-vapour coexisting regions of n-pentane confined in slits of 17, 13 and 9 Å. The critical temperature of the liquid-vapour coexistence shifts to lower temperatures upon confining and we can therefore conclude that our simulations for measuring the solvation force, were sufficiently far from the critical point.

References

[1] J.D. van der Waals, in Ph.D thesis, Hoogeschool te Leiden, The Netherlands, 1873.
[2] E.J.W. Verwey, J.Th.G. Overbeek (eds.), in Theory of Stability of Lyophobic Colloid, Elsevier, Amsterdam, 1948.
[3] J.N. Israelachvili (ed.), in Intermolecular and Surface Forces, Academic Press, New York, 2nd edn., 1992.
[4] J.N. Israelachvili, Acc. Chem. Res. 20 (1987) 415.
[5] J.E. Lane, T.H. Spurling, Aust. J. Chem. 34 (1981) 1529.
[6] I.K. Snook, W. van Megen, J. Chem. Phys. 72 (1980) 2907.
[7] W. van Megen, I.K. Snook, J. Chem. Phys. 74 (1981) 1409.
[8] J.J. Magda, M. Tirell, H.T. Davis, J. Chem. Phys. 83 (1985) 1888.
[9] D. Henderson, M. Lozada-Cassou, J. Colloid Interface Sci. 114 (1986) 180.
[10] M. Schoen, D.J. Diestler, J.H. Cushman, J. Chem. Phys. 87 (1987) 5464.
[11] M. Schoen, J.H. Cushman, D.J. Diestler, C.L. Rhykerd Jr., J. Chem. Phys. 88 (1988) 1394.
[12] A.Z. Panagiotopoulos, Mol. Phys. 62 (1987) 701.
[13] P. Tarazona, U. Marini Bettolo Marconi, R. Evans, Mol. Phys. 60 (1987) 573.
[14] B.K. Peterson, K.E. Gubbins, Mol. Phys. 62 (1987) 215.
[15] B.K. Peterson, K.E. Gubbins, G.S. Heffelfinger, U. Marini Bettolo Marconi, F. van Swol, J. Chem. Phys. 88 (1988) 6487.
[16] J.P.R.B. Walton, N. Quirke, Mol. Simulation 2 (1989) 361.
[17] T.K. Vanderlick, L.E. Scrivens, H.T. Davis, J. Chem. Phys. 90 (1989) 2422.
[18] D.J. Courtemanche, T.A. Pasmore, F. van Swol, Mol. Phys. 80 (1993) 861.
[19] J.N. Israelachvili, S.J. Kott, M.L. Gee, T.A. Witten, Macromolecules 22 (1989) 4247.
[20] H.K. Christenson, D.W.R. Gruen, R.G. Horn, J.N. Israelachvili, J. Chem. Phys. 87 (1987) 1834.
[21] R.G. Horn, J.N. Israelachvili, Macromolecules 22 (1988) 4253.
[22] J.N. Israelachvili, S.J. Kott, J. Chem. Phys. 88 (1988) 7162.
[23] Y. Wang, K. Hill, J.G. Harris, J. Chem. Phys. 100 (1994) 3276.
[24] S. Granick, A.L. Demirel, L.L. Cai, J. Peanasky, Israel J. Chem. 35 (1995) 75.
[25] J.P. Gao, W.D. Luedtke, U. Landman, J. Chem. Phys. 106 (1997) 4309.
[26] R. Evans, U. Marini Bettolo Marconi, J. Chem. Phys. 86 (1987) 7138.
[27] J.R. Henderson, Mol. Phys. 59 (1986) 89.
[28] D. Frenkel, B. Smit (eds.), in Understanding Molecular Simulation: From Algorithms to Applications, Academic Press, New York, 1996.
[29] M.P. Allen, D.J. Tildesley (eds.), in Computer simulation of liquids, Clarendon Press, Oxford, 1994.
[30] B. Smit, S. Karaborni, J.I. Siepmann, J. Chem. Phys. 102 (1995) 2126.
[31] W.A. Steele, Surf. Sci. 36 (1973) 317.
[32] P. Padilla, S. Toxvaerd, J. Chem. Phys. 101 (1994) 1490.
[33] M. Dijkstra, J. Chem. Phys. 107 (1997) 3277.
[34] D. Frenkel, G.C.A.M. Mooij, B. Smit, J. Phys. Condens. Matter 4 (1992) 3053.
[35] S. Balasubramanian, M.L. Klein, J.I. Siepmann, J. Phys. Chem. 100 (1996) 11960.
[36] R. Evans, U. Marini Bettolo Marconi, P. Tarazona, J. Chem. Phys. 84 (1986) 2376.